Acta Montanistica Slovaca
ISSN 1335-1788
actamont.tuke.sk

Observations of the oil-polluted soil of Absheron Peninsula using Landsat 8 OLI and Sentinel 2A imagery

Saddam HASHIMOV[1] *and Jarosław ZAWADZKI*[2]*

Authors' affiliations and addresses:
[1] Warsaw University of Technology, Faculty of Building Services, Hydro and Environmental Engineering, Nowowiejska 20, 00-661 Warszawa, Poland
e-mail: hashimov644@gmail.com

[2] Warsaw University of Technology, Faculty of Building Services, Hydro and Environmental Engineering, Nowowiejska 20, 00-661 Warszawa, Poland
e-mail: jaroslaw.zawadzki@pw.edu.pl

***Correspondence:**
Jarosław Zawadzki, Warsaw University of Technology, Faculty of Building Services, Hydro and Environmental Engineering, Nowowiejska 20, 00-661 Warszawa, Poland
tel.: +48 22 660-5426
e-mail: jaroslaw.zawadzki@pw.edu.pl

Funding information:
Statutory activities of Warsaw University of Technology, Faculty of Building Services, Hydro and Environmental Engineering, Poland

Acknowledgement:
The authors would like to thank dr inż. Jan Bogacki from the Faculty of Building Services, Hydro and Environmental Engineering at Warsaw University of Technology for the help in laboratory measurements.

How to cite this article:
Hashimov, S. and Zawadzki, J. (2022) Observations of the oil-polluted soil of Absheron Peninsula using Landsat 8 OLI and Sentinel 2A imagery. *Acta Montanistica Slovaca,* Volume 27 (3), 607-619.

DOI:
https://doi.org/10.46544/AMS.v27i3.04

Abstract
The Absheron Peninsula is the biggest urbanized area in Azerbaijan. Along with the growth of the massive oil production, the role of the Peninsula has increased, and big ecological problems have arisen.
In this research, the investigation of the possibility of detecting hydrocarbons in sandy soil through Landsat 8 OLI and Sentinel 2 A satellite and drone images and chemical analysis was conducted. The main study was based on the satellite imagery of Landsat 8 OLI and Sentinel 2A, employing NDVI calculations and analyses. In order to calculate NDVI, ESRI ArcGIS 10.3 software has been used. The multispectral images with 30m spatial resolution of Landsat 8 and 10 m resolution multispectral images of Sentinel 2 were used. Additionally, drone observations lead to obtaining high-resolution data about soil pollution in the study area. Also, field samples were taken to the laboratory, and necessary chemical analysis was performed for validation purposes.
This study showed that multispectral remote sensing can be used to detect hydrocarbons in the soil in oil production areas. Hydrocarbon-bearing substances' absorption into the soil results in a low value of NDVI in the study area. The observations in the winter and summer seasons show that the seasonal changes in weather conditions affect both the amount of oil contamination in the soil and the detection process of soil pollution by oil using remote sensing.

Keywords
Remote Sensing, NDVI, Landsat 8, Sentinel 2, Oil spill, Hydrocarbon detection, Absheron Peninsula, Azerbaijan

Introduction

Oil production has occupied a major role in Azerbaijan's economy (Feyzullayev and Ibragimov, 2014; Khalilova, 2014; Pivin et al., 2014; Sharov et al., 2019). The Absheron Peninsula is located on the west coast of the Caspian Sea in Azerbaijan (Fig.1). Except for the capital city of Baku, there are there 32 smaller settlements and one big city (Abd Ali et al., 2021). The administrative area of the region is 1407.5 km^2. About 40% country's industrial enterprises are concentrated in the Absheron Peninsula. The foundation of its economy is oil and gas extraction and their processing and related industry, including mainly petrochemical, chemical, mechanical, and electricity production, as well as metallurgy (Burduk et al., 2021). The Absheron Peninsula plays an important role in processing a large number of black and non-ferrous metals, wood, building materials, and the food industry. Moreover, the important oil and gas pipelines are located there (Kopas et al., 2017). However, it must be noted that the major amount of oil production lasting more than 150 years has brought enormous ecological problems to the Absheron Peninsula, especially considering the soil status (Baghirova, 2020; Bayramli, 2020; Bektashi and Cherp, 2002). Oil and oil products are soil pollutants with the highest priority due to their toxicity, spreading scale, and high migration ability (Wiecek et al., 2019). Oil fields' development and exploitation and violation of the hydrocarbon transportation rules resulted in the pollution of the natural ecosystem(Kopas et al., 2017). Oil-contaminated soil and water created during oil and gas extraction pose a great danger to the population.

This study focuses on remote sensing observation methods and the detection of soil contamination with oil in the Absheron Peninsula by remote sensing (Handrik et al., 2017). In the past years, remote sensing observation and detection of oil contamination and spillage have gained popularity in water and soil pollution detection mainly due to their cheapness and large spatial coverage (Hacke et al., 2012; Karkush et al., 2014; Adamu et al., 2016; Fingas and Brown, 2017; Kaplan et al., 2022.; Laššák, et al., 2020; Blišťan et al., 2021; Kovanič et al., 2021). Remote sensing is indispensable for ecological and conservation applications (Kovanič et al., 2021, Blistanova et al., 2014, Blistanova et al., 2015). Remote sensing is indispensable for ecological and conservation applications and will play an increasingly important role in the future (Dodge and Congalton, 2013; Baghdadi and Zribi, M., 2016). For many purposes, it provides the only means of measuring the characteristics of habitats across broad areas and detecting environmental changes that occur as a result of human or natural processes (The Sentinel missions, 2022). These data are increasingly easy to find and use. Although field and remote sensing data are often collected at divergent spatial scales, ecologists have begun to recognize both the potential and the pitfalls of satellite information. Established remote sensing systems provide opportunities to develop and apply new measurements of ecosystem function across landscapes and regions (Kerr and Ostrovsky, 2003).

The main purposes of this study are:

1. The observation of the soil contamination by oil products and its eventual seasonal changes in the Absheron Peninsula by Landsat 8 OLI and Sentinel 2A satellites in the winter and summer seasons.
2. Comparison of usefulness of Landsat 8 OLI and Sentinel 2A satellite imagery regarding the observation of soil contamination by oil.
3. The investigation of NDVI changes caused by soil contamination with oil at the research area.

Thus, this study could give practical insight into the discussed problem to Azerbaijan oil companies.

Material and Methods

Study area

The study area is chosen in the Absheron Peninsula, located mainly in Baku city (Fig.1).

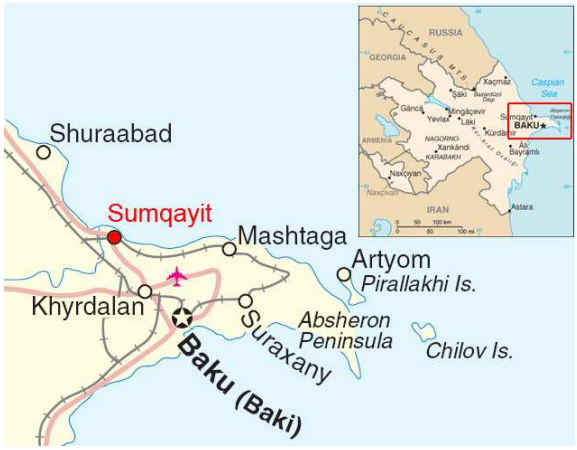

Fig.1. Absheron Peninsula with its municipalities. (Baku, Wikipedia, 2022)

The Absheron Peninsula soils are partly salty and saline grey and grey-brown soils. The granulometric composition of the soils can be medium-clay, clay, and in the eastern part of the peninsula, medium-clay sand (Kuric et al., 2022). The soils of Absheron Peninsula are exposed to high soil erosion due to winds and irrigation. The Absheron Peninsula has a temperate semi-arid climate (Köppen climate classification BSk) (Belda et al., 2014) with warm and dry summers, cool and occasionally wet winters, and strong winds throughout the whole year (Kuric et al., 2021). The annual sum of sunny hours amounts to 2200 -2400.

More specifically, the study area is situated in the north coastal area of Boyukshor Lake (Fig.2). Boyukshor Lake is located 4 m above sea level, in the middle of the Absheron Peninsula. The surface area of the lake is 1300 ha, and the volume of water is 47.3 million m^3. All wastewater near factories and residential areas is discharged to Boyukshor Lake. Water samples taken from the lake show that the lake water is polluted and mineralized more than the norm (120g/l) (Hacke et al., 2012). Lack of oxygen has been observed in the lake water; it is caused by the oxidation process of pollutants thrown in the lake. The concentrations of phenol and petroleum products are 20 and 66 times more than the norm (Hacke et al., 2012). Although some actions have been taken, part of Boyukshor Lake is drained for treatment (Kuric et al., 2020). The pollution level is still very high, and the contamination process is still ongoing (Muravev et al., 2019). The study area was divided into 2 zones, northern and southern, close to each other and denoted furthermore as Area #1 and Area #2, respectively (Fig. 2, yellow contours). The surface of the first area is approx. 40.5 hm^2 and the second area is approx. 26 hm^2.

Fig. 2. The specific study area is composed of two contaminated areas Northern and Southern, close to each other. They are delineated using yellow lines and denoted furthermore as to Area #1 and Area #2. The points where samples were taken from the research area are also shown. Coordinates of the areas are : #1) 40°26'40.6"N 49°54'34.3"E , #2) 40°26'34.3"N 49°54'30.3"E

Data sets and methodology

The analysis was completed using ESRI's ArcGIS 10.3 and Google Earth Pro software, a high-resolution Drone image. Six soil samples have been taken from the research area by the author to prove the usability of satellite images in case of determination of oil spill and contamination in the soil. The dataset consists of two satellites, Landsat 8 OLI and Sentinel 2A images. All computations have been done based on NDVI calculation. Detailed information about datasets is given below.

Landsat 8 OLI

In order to get the required data from the Landsat satellite, Landsat 8 OLI data (Landsat Levels of Processing, 2022) has been downloaded from the website of the USGS government agency. The datasets include two different seasons, winter (Saga el al., 2014), and summer. Two different time series datasets help to get the more accurate result during the research process (Saga 2009). The spatial resolution of the Landsat 8 imagery is 30 m, meaning that one pixel in the imagery represents 30 m on the ground.

Sentinel 2A

As mentioned earlier, the supplier of the second dataset is the satellite Sentinel 2A. In this research, the Sentinel 2A dataset has been downloaded from the EO Browser website (Saga et al., 2014). The spatial resolution of Sentinel 2A is 10m in the multispectral band, which will be used in the research. As in Landsat 8, the dataset here is also has been taken in two separate seasons (Sapietova , et al., 2011). The datasets cover the winter (31.01.2018) and summer (10.07.2018) seasons.

Drone Image

In order to determine the contamination areas more accurately, a high-resolution drone image has been used. This data has been obtained from the Caspian Geomatics environment agency. The Caspian Geomatics LTD created conditions for the use of a database (Segota et al., 2020). The spatial resolution of this drone image is 10 cm. This data has mostly been used to determine and measure the contamination area (Tlach et al., 2019), appoint additional objects and resources in the research area, and for the estimation of the final result of images of satellites. Detailed information about drone images is given in Tab.1.

Tab. 1. Drone image parameters

Entity ID	Boyukshor_1
Agency	Caspian Geomatics LTD
Datum	WGS84
Map Projection	UTM
UTM Zone	39N
Resolution	10
Unit	Centimetre

NDVI calculations

All these datasets have been carefully analyzed, and then NDVI was calculated by using ESRI's ArcGIS 10.3 software using the following formula (Carlson and Ripley,1997; Arellano et al., 2015; Pałaś and Zawadzki, 2020):

$$NDVI = \frac{NIR-RED}{NIR+RED}. \quad (1)$$

Specifically, the NDVI calculation process involved creating a normalized difference vegetation index for the Landsat 8 OLI (Band 5(NIR)-Band 4(RED)/Band 5(NIR)+Band 4(RED)) and Sentinel 2A (Band 8(NIR)-Band 4(RED)/Band 8(NIR)+Band 4(RED)) (Ke et al., 2015; Bezerra et al., 2018; Sentinel-2: Satellite imagery, 2022).

Tab.2. Landsat 8 and Sentinel-2 spectral bands definition and spatial resolutions used for NDVI calculations

	Central wavelength [µm]	Spatial resolution [m]
Landsat 8 bands		
Band 4-RED	0.636-0.673	30
Band 5-NIR	0.851-0.879	30
Sentinel-2A bands		
Band 4-RED	0.665	10
Band 8-NIR	0.842	10

Sentinel 2A satellite is also able to achieve a 10-meter resolution for NIR in BAND 8. This is a reason for using BAND 8 instead of BAND 5, unlike Landsat 8.

Software

To conduct NDVI calculation of all datasets, ESRI ArcGIS 10.3 software has been used. In addition, Google Earth Pro software has been used to determine climate effects in the research area and analyze these changes.

Work process

In the first step, in order to locate and detect the occurrence of oil spillage and extension of the contaminated area, high-resolution Drone images have been used (Zajacko et al., 2020). The oil spill in the north part of the coastline of Boyukshor Lake was studied for two different seasons (winter and summer) of the year 2018. Additionally, two Google earth images, in the dates of 19.01.2018 and 14.07.2018, have been downloaded for each season to check the accuracy of the satellite data.

In the second step, two Landsat 8 OLI and two Sentinel 2A images have been downloaded for the winter and summer seasons. In the next step, the studied area has been marked and clipped off by using ArcGis 10.3 software tools to prepare the NDVI calculation process. Then, a soil classification map was made by using a high-resolution drone image to determine the oil-contaminated area.

The next process was chemical analyses. The six polluted and non-polluted soil samples were analyzed in the laboratory. Chemical analyses were then used to validate satellite observations.

In the final step, e.g., after finishing all calculations and analyses, all satellite results were compared with laboratory measurements in order to check the accuracy of the satellite observations.

Fieldwork and laboratory research

Oil contamination can affect the physical and chemical properties of soil. Hydrocarbon contamination can also increase soil total organic carbon content in the soil and change pH values and other chemical properties of soil.

Six samples were collected from polluted and non-polluted areas to analyze the physicochemical properties of the soil (Fig.2).

The class (contaminated/uncontaminated) and the coordinates of the samples taken from the area are given in Tab.3

Tab. 3. Coordinates and class of the taken samples

No.	Latitude	Longitude	Class
Sample 1	40°26'42.50"N	49°54'30.70"E	Contaminated
Sample 2	40°26'46.19"N	49°54'25.36"E	Contaminated
Sample 3	40°26'42.66"N	49°54'27.02"E	Contaminated
Sample 4	40°26'39.37"N	49°54'34.47"E	Contaminated
Sample 5	40°26'34.99"N	49°54'28.74"E	Contaminated
Sample 6	40°26'43.01"N	49°54'21.90"E	Uncontaminated

The preparation of soil samples for the petroleum compounds determination is based on extracting organic compounds with dichloromethane (DCM) in a Soxhlet extractor before mass analysis. The aim of the extraction is to transfer organic micropollutants from the solid sample into the solvent. DCM is a very strong extraction agent. It can extract a large variety of compounds from a sample – both petroleum and not petroleum-based substances. The unwanted substances have to be removed during the purification process. Afterwards, the sample must be evaporated at ambient temperature. The content of petroleum-based compounds was determined as a difference in weighing bottle masses before and after evaporated extract collection.

Results and discussion

Hereafter, detailed images of the research area are presented. Fig. 3 shows the high-resolution drone image of the study area.

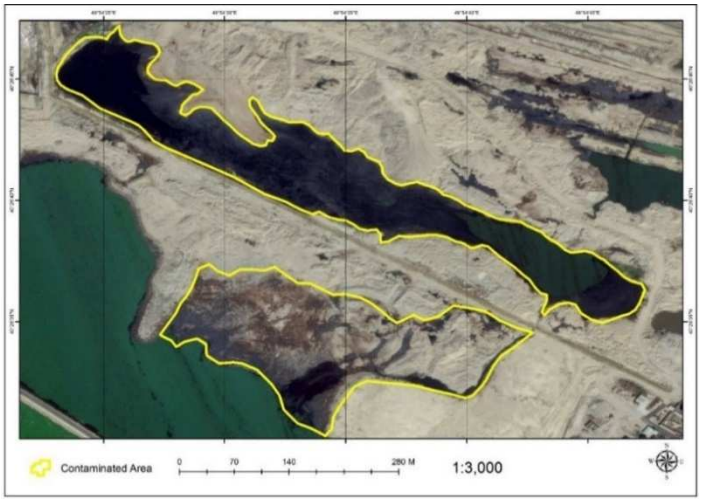

Fig. 3. The high-resolution drone image of the study area with contaminated places marked with the yellow line

Fig. 4 shows the map of all objects and polluted zones in the research area obtained using a high-resolution drone image. The map delivers the exact information about the polluted area, including water, vegetation, urbanized area, etc. The contaminated area is delineated using a dark brown contour, while water, urban, and vegetation area is delineated using blue, pink, and green colour lines, respectively.

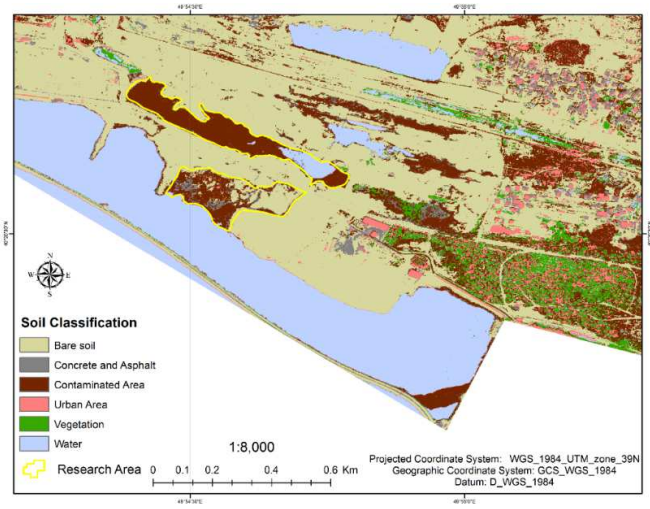

Fig. 4. Soil classification map of the research area

Figs 5 and 6 represent True Color images of the contaminated area which have been taken by Landsat 8 OLI and Sentinel 2A during the winter season, while Figs 7 and 8 demonstrate True Color images of Landsat 8 OLI and Sentinel 2A in summer. The red and green outlines in the given imagery are contamination and vegetation areas, respectively. In contrast to the situation shown in Figs 5 and 7, it is possible to see the clearly contaminated and vegetation areas in Figures 6 and 8, obtained from10 m spatial resolution imagery of Landsat 8 OLI.

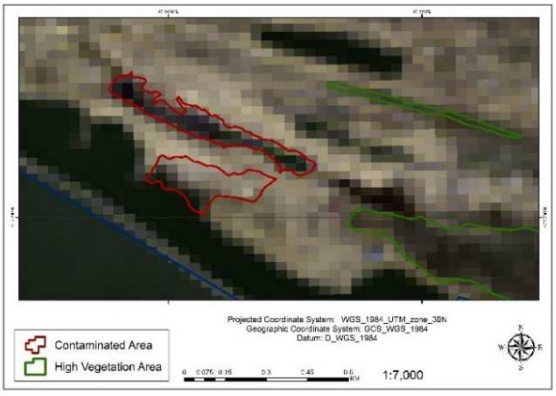

Fig. 5. Landsat 8 OLI, True Color Imagery of the study area. The True Color Image is obtained from Landsat 8 OLI in the winter season with 30 m spatial resolution. Date: 31.01.2018

Fig. 6. Sentinel 2A, True Color Imagery of the study area. The True Color Image is obtained from Sentinel 2A in the winter with 10 m spatial resolution. Date: 31.01.2018

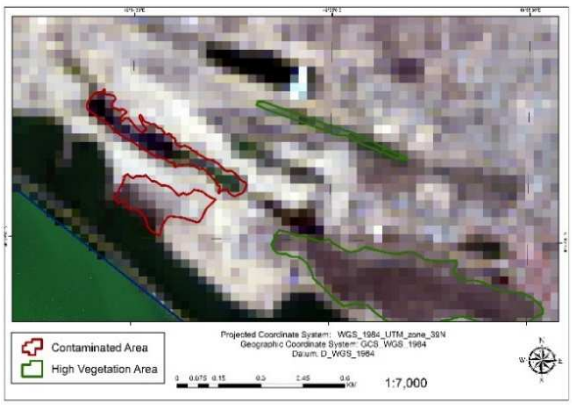

Fig. 7. Landsat 8 OLI, True Color Imagery of the study area. The True Color Image is obtained from Landsat 8 OLI in the summer season with 30 m spatial resolution. Date: 10.07.2018

Fig. 8. Sentinel 2, True Color Imagery of the study area. The True Color Image is obtained from Sentinel 2A in the summer season with 10 m spatial resolution. Date: 10.07.2018

As was explained above, NDVI is commonly used to identify vegetation state. However, this research is used to determine oil-contaminated soil in the study area.

After NDVI calculation using Landsat 8 OLI and Sentinel 2A datasets, the following results have been obtained. As can be seen, there are different values of NDVI ranging between -1 and +1.

It is important to stress that in the figures in this paper, the red colour demonstrates highly contaminated areas while the green colour indicates high vegetation areas. The rest shades of yellow colour on the map show bare soil, which is less contaminated. The detailed soil classification map is given above in Fig. 4.

As can be seen from the figures below, there are noticeable differences between the results of Landsat 8 OLI and Sentinel 2A. Fig. 9 demonstrates NDVI results obtained from Landsat 8 OLI satellite imagery on the study area during the winter season. The maximum value of NDVI was approximately 0.63, while the minimum one was -1.18. However, it can be stated that the overall pollution here is relatively low. This is caused by a high amount of winter precipitation that affects the chemical properties of the soil. In Area #2 (the southern one), more than 10 m^2 has been covered by water as a result of the increased water level. Additionally, when analyzing NDVI, it should be taken into account the rather low resolution of Landsat 8 OLI of 30 m, which is clearly visible in Fig.9.

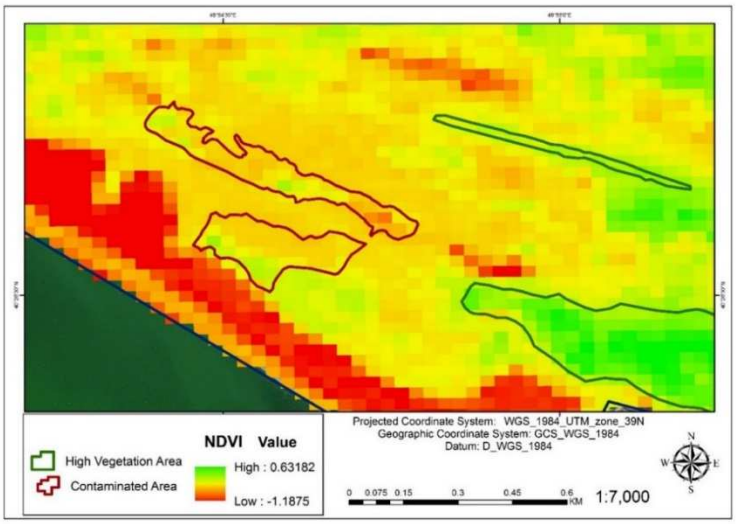

Fig. 9. NDVI distribution obtained by Landsat 8 OLI imagery in the winter season. The contamination areas are not delineated precisely because of low spatial resolution and winter conditions. Date: 31.01.2018

In Fig. 10, the NDVI values change approximately between -0.28 and 0.56. Unlike Landsat 8 OLI, the result obtained from Sentinel 2A in the winter season is quite enough to observe the pollution in the field area. The amount of contamination in Area #1 (the northern one) is seen as considerable. Again, the effect of seasonal changes can be observed in Area #1 (the southern one).

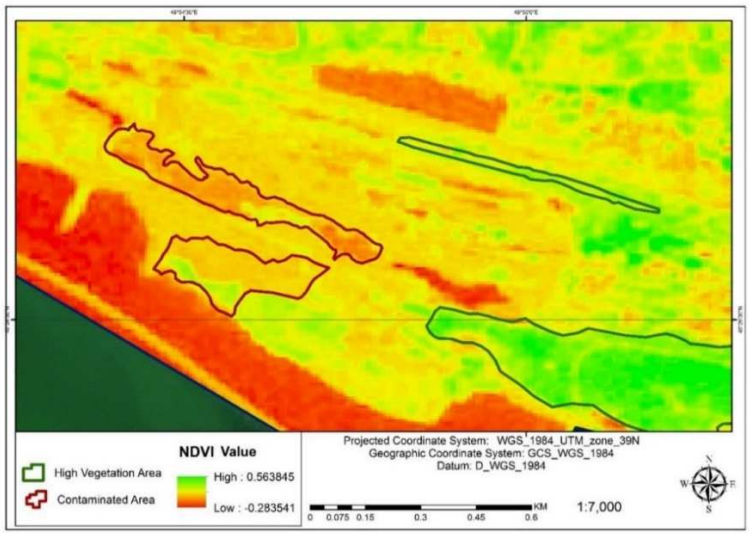

Fig. 10. NDVI distribution obtained by Sentinel 2 imagery in the winter season. The polluted area is clearly seen in Area #1 (the northern one). However, the rise of the water level in Area #2 (the southern one) does not allow for precise determination of the contamination area

Fig. 11 presents the NDVI distribution of Landsat 8 OLI in the study area in the summer season. Contrary to the winter season, the soil contamination obtained from Landsat 8 OLI for the summer season is visibly higher. The temperatures reaching 31^0 Celsius in the summer cause evaporation of all amounts of water from the research area, and only the oil contamination is left behind. This process directly affects the determination of satellite observations. In Area #2, it was not possible to precisely delineate soil pollution because of the relatively low Landsat 8 OLI resolution.

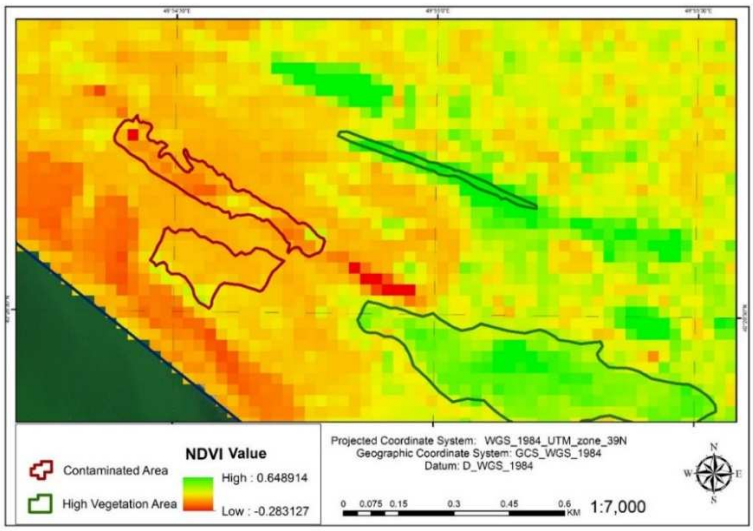

Fig. 11. NDVI distribution obtained by Landsat 8 OLI imagery in the summer season. Soil contamination by petroleum products in Areas #1 and #2 is clearly higher than in the winter season. Soil contamination in Area #2 is difficult for precise delineation because of the relatively low spatial resolution of Landsat 8 OLI. Date: 10.07.2018

The last Figure 12 for NDVI calculation illustrates the Sentinel 2A satellite result for the summer season on 10.07.2018. The NDVI values change between -0.19 and 0.59. Sentinel 2A uses the 10x10m spatial resolution, which identifies the contamination area as considerable. Although the pollution is low, the Sentinel 2A satellite was able to identify the contamination in the coastal area, which belongs to our second research area.

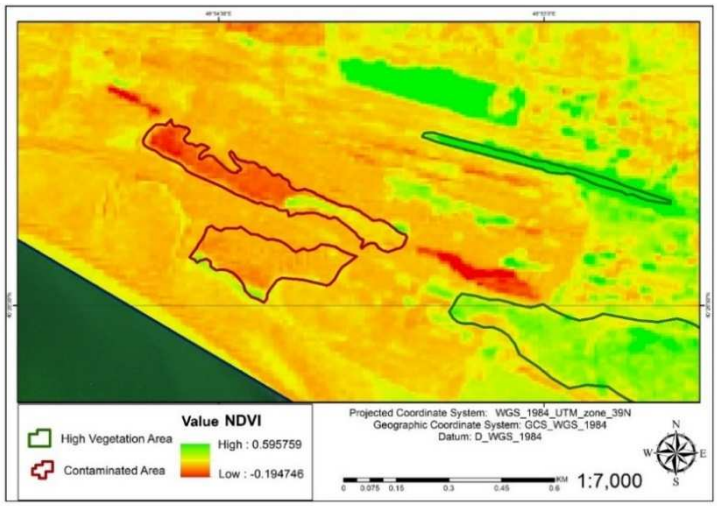

Fig. 12. NDVI distribution obtained by Sentinel 2 imagery in the summer season. Date: 10.07.2018

In summary, one can see in the last four figures (Figs 9-12) the superiority of Sentinel 2A imagery over Landsat 8 OLI one. Using the Sentinel 2A satellite, it was possible to determine soil pollution with oil as well as to observe its changes related to the seasons.

For validation purposes, the content of hydrocarbon in the collected soil samples was determined in the laboratory. Fig. 13 presents the histogram of the content of hydrocarbon in mg per kilogram in the studied contaminated samples in the summer season. The blue bars demonstrate the hydrocarbon content in the samples taken from contaminated area while the orange line in the sample is taken from a relatively clean place. In the latter sample, the content of hydrocarbon was 1267 mg/kg. The highest contamination value has been observed in Sample 2, namely 67283 mg/kg (Figs 13, 14). Thus, the pollution of the site considered to be clean was only about 2% of that of the most polluted site.

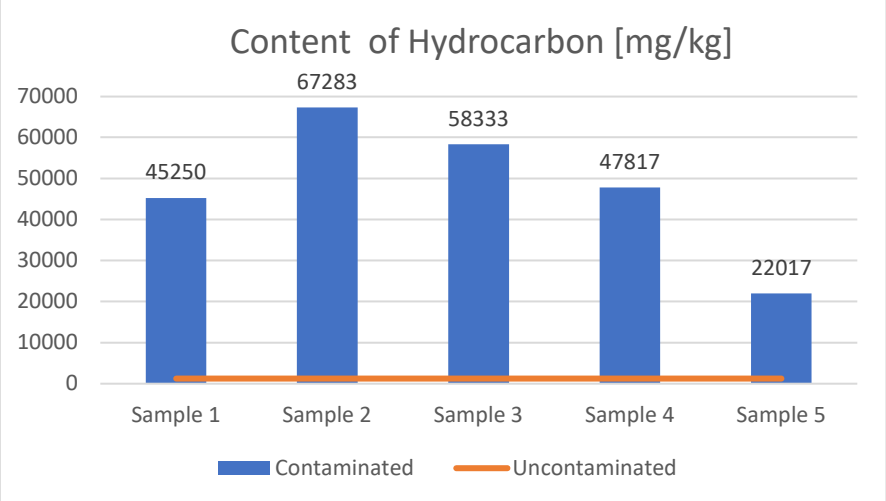

Fig.13. Graph of the content of hydrocarbon mg/kg in studied soil samples

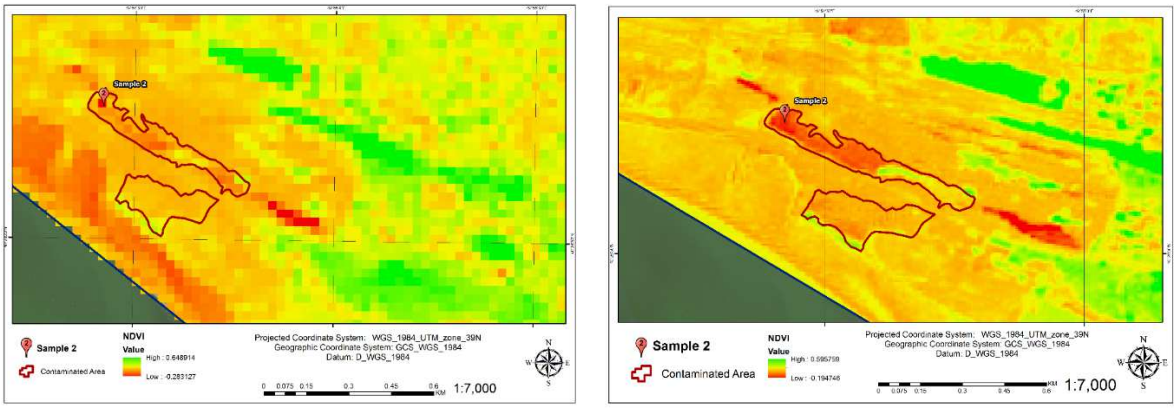

Fig.14. The location of Sample 2 point on the NDVI spatial distribution obtained using Landsat 8 OLI (left) and Sentinel 2A (right) imagery in the summer season

As we can see in Fig. 14, Sample 2 was taken from the place lying on the border of two Landsat 8 OLI pixels, whereas the pollution level estimated from Sentinel 2A imagery around this place is much more continuous, which enables more accurate validation and estimation.

In order to determine the statistical relationship between NDVI calculated based on Landsat 8 OLI and Sentinel 2A satellite imagery and hydrocarbon content in soil Pearson's correlation coefficient has been calculated using NDVI and validation measurements. Fig.15 shows an exemplary relationship between these variables on July 7, 2018.

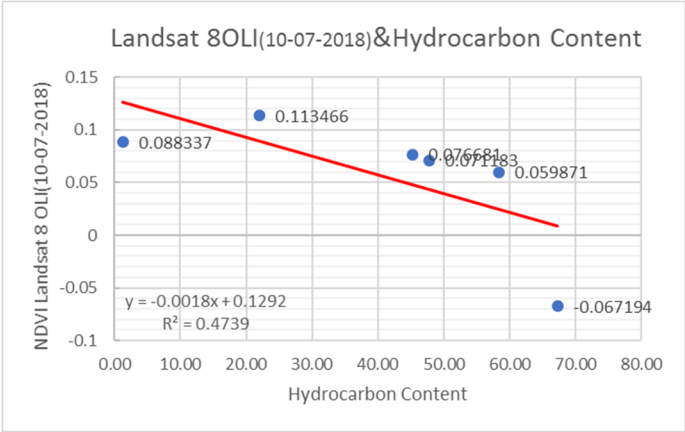

Fig.15. Scatter plot and regression line between NDVI obtained from Landsat 8 OLI satellite in the summer season [Landsat 8OLI (10-07-2018)] and hydrocarbon content in the soil samples

As shown in Fig.15, the clear dependence between NDVI and the hydrocarbon content in the soil samples exists. Pearson's correlation coefficient based on this regression line is relatively high in absolute value and negative (- 0.69). This indicates that when NDVI values decrease, the amount of hydrocarbon content increases.

Conclusions

This study demonstrates the usefulness of satellite observations supported by drone images and validation field measurements to identify oil-polluted soils in semi-desert and dry climates of the Absheron Peninsula. Two different satellite datasets, namely those of Landsat 8 and Sentinel 2, were compared for the possible application in similar studies. NDVI was used for the delineation of oil-polluted areas. The specific conclusions related to the study are as follows.

1. The satellite image analyses validated by laboratory analyses show that NDVI could be considered an indicator of soil pollution with oil on the Absheron Peninsula.
2. The use of ESA's Sentinel 2A satellite was more conclusive in this study than Landsat 8 OLI. This is because the Sentinel 2A satellite has higher spatial resolution than Landsat 8 OLI.

3. The seasonal surveillance and in-situ measurements on the study area by satellite images proved the effect of seasonal changes in soil pollution with oil. Remote sensing observations suggest that the amount of precipitation has an important effect on petroleum pollution in the soil.
4. Pearson's correlation coefficients between NDVI values and hydrocarbon content in soil determined on the basis of fieldwork are reasonably high and negative.

References

Abd Ali, L.M., Ali, Q.A., Klačková, I., Issa, H.A., Yakimovich, B.A., Kuvshimov, V. (2021). Developing a thermal design for steam power plants by using concentrating solar power technologies for a clean environment. Acta Montanistica Slovaca, vol. 26 (4), 2021, pp. 773-783, 2021, DOI https://doi.org/10.46544/AMS.v26i4.14, 2021

Absheron Peninsula. Wikipedia. Available at: https://en.wikipedia.org/wiki/Absheron_Peninsula (Accessed June 14, 2022).

Adamu, B., Tansey, K. and; Ogutu, B., 2016. An investigation into the factors influencing the detectability of oil spills using spectral indices in an oil-polluted environment. International Journal of Remote Sensing, 37(10), pp.2338–2357.

Arellano, P., Tansey, K., Balzter, H., and Boyd, D. S. (2015). Detecting the effects of hydrocarbon pollution in the Amazon forest using hyperspectral satellite images. Environmental pollution (Barking, Essex : 1987), 205, 225–239. https://doi.org/10.1016/j.envpol.2015.05.041

Baghdadi, N. and Zribi, M., 2016. Land Surface Remote Sensing: Environment and risks, London England: ISTE Press.

Baghirova, S.H.A.F.A.Q., 2020. Complex research of environmental problems in the Absheron Peninsula, S.l.: LAP Lambert Academic Publ.

Baku, Wikipedia. Available at: https://en.wikipedia.org/wiki/Baku (Accessed June 14, 2022).

Bayramli, G., 2020. The environmental problems of Azerbaijan and the search for solutions. Wseas Transactions on environment and development, 16, pp.423–433.

Belda, M. et al., 2014. Climate classification revisited: From köppen to trewartha. Climate Research, 59(1), pp.1–13.

Bektashi, L. and Cherp, A., 2002. Evolution and current state of Environmental Assessment in Azerbaijan. Impact Assessment and Project Appraisal, 20(4), pp.253–263.

Bezerra, U.A. et al., 2018. Comparison of the normalized difference vegetation index (NDVI) between the sensors OLI-LANDSAT satellite-8 and MSI-sentinel-2 satellite in Semi-Arid Region. Anuário do Instituto de Geociências - UFRJ, 41(3), pp.167–177.

Blistan, P.; Kovanič, L.; Patera, M.; Hurčík, T. Evaluation quality parameters of DEM generated with low-cost UAV photogrammetry and Structure-from-Motion (SfM) approach for topographic surveying of small areas. Acta Montan. Slovaca 2019, 24, 198–212.

Blistanova, M.; Katalinic, B.; Kiss, I.; Wessely, E. Data preparation for logistic modeling of flood crisis management. Procedia Engineering, 2014 Conference paper, 2p, DOI: 10.1016/j.proeng.2014.03.151

Blišťanová, M., Blišťan, P. and Blažek, J. Mapping of surface objects and phenomena using unmanned aerial vehicle for the purposes of crisis. In: SGEM 2015. P. 491-499. - ISBN 978-619-7105-39-1 - ISSN 1314-2704

Burduk, A., Wiecek, D., Tlach, V., Ságová, Z., Kochanska, J. (2021). Risk assessment of horizontal transport system in a copper mine. Acta Montanistica Slovaca, vol. 26 (2), 2021, DOI 10.46544/AMS.v26i2.09, 2021

Carlson, T.N. and Ripley, D.A., 1997. On the relation between NDVI, fractional vegetation cover, and Leaf Area index. Remote Sensing of Environment, 62(3), pp.241–252.

Dodge, R.L. and Congalton, R.G., 2013. Meeting environmental challenges with remote sensing imagery, Alexandria, VA: American Geosciences Institute.

Feyzullayev, A.A. and Ibragimov, V.B., 2014. Environmental consequences of long-term development of petroleum fields, Absheron P-La, Azerbaijan, case history. Journal of Environmental Protection, 05(17), pp.1603–1610.

Fingas, M. and Brown, C. (2017). A Review of Oil Spill Remote Sensing. Sensors 18, 91. https://doi.org/10.3390/s18010091

Hacke, E., Maes, F., and Schoukens, H. (2012). Oil spill detection by remote sensing: a comparative legal analysis. https://lib.ugent.be/catalog/rug01:001891945

Handrik, M., Kopas, P., Baniari, V., Vasko, M., Saga, M. (2017). Analysis of stress and strain of fatigue specimens localised in the cross-sectional area of the gauge section testing on bi-axial fatigue machine loaded in the high-cycle fatigue region. XXI Polish-Slovak Scientific Conference Machine Modeling and Simulations MMS 2016, Hucisko, Poland, 6-8 sept. 2016, Procedia Engineering, vol. 177, pp. 516-519, DOI 10.1016/j.proeng.2017.02.254, 2017

Kaplan, G. et al., 2022. Oil-contaminated soil modeling and remediation monitoring in arid areas using remote sensing. *Remote Sensing*, 14(10), p.2500.

Karkush, M.O., Ziboon, A.T., and Hussien, H.M. (2014). Studying the Effects of Contamination on Soil Properties Using Remote Sensing. The Journal of Engineering, 20, 78-90.

Ke, Y. et al., 2015. Characteristics of landsat 8 OLI-derived NDVI by comparison with multiple satellite sensors and in-situ observations. Remote Sensing of Environment, 164, pp.298–313.

Kerr, J.T., and Ostrovsky M. (2003) From space to species: ecological applications for remote sensing. Trends in Ecology & Evolution 18(6) p.299-305. https://doi.org/10.1016/S0169-5347(03)00071-5

Klarák, J., Andok, R., Hricko, J., Klačková, I., Tsai, H.-Y. (2022). Design of the Automated Calibration Process for an Experimental Laser Inspection Stand. Sensors 2022, 22, 5306, https://doi.org/10.3390/s22145306, 2022

Kopas, P., Blatnicky M., Saga M., Vasko, M. (2017). Identification of mechanical properties of weld joints of AlMgSi07.F25 Aluminium Alloy. Metalurgija, vol. 56 (1-2), 2017, pp. 99-102, 2017

Kopas, P., Saga, M., Baniari, V., Vasko, M., Handrik, M. (2017). A plastic strain and stress analysis of bending and torsion fatigue specimens in the low-cycle fatigue region using the finite element methods. XXI Polish-Slovak Scientific Conference Machine Modeling and Simulations MMS 2016, Hucisko, Poland, 6-8 sept. 2016, Procedia Engineering, vol. 177, pp. 526-531, DOI 10.1016/j.proeng.2017.02.256, 2017

Kovanič, Ľ.; Blistan, P.; Štroner, M.; Urban, R.; Blistanova, M. Suitability of Aerial Photogrammetry for Dump Documentation and Volume Determination in Large Areas. *Appl. Sci.* 2021, *11*, 6564. https://doi.org/10.3390/app11146564

Kovanič, Ľ., Blistan, P., Rozložník, M. and Szabó, G. UAS RTK / PPK photogrammetry as a tool for mapping the urbanized landscape, creating thematic maps, situation plans and DEM. Acta Montanistica Slovaca. 2021, Volume 26 (4) 649-660 DOI: https://doi.org/10.46544/AMS.v26i4.05

Kovanič, Ľ.; Blistan, P.; Urban, R.; Štroner, M.; Blišťanová, M.; Bartoš, K.; Pukanská, K. Analysis of the Suitability of High-Resolution DEM Obtained Using ALS and UAS (SfM) for the Identification of Changes and Monitoring the Development of Selected Geohazards in the Alpine Environment—A Case Study in High Tatras, Slovakia. *Remote Sens.* 2020, 12, 3901, doi:10.3390/rs12233901.

Kuric, I., Klačková, I., Domnina, K., Stenchlák, V., Sága, M. jr. (2022). Implementation of Predictive Models in Industrial Machines with Proposed Automatic Adaptation Algorithm. Applied Sciences - Basel, Mdpi, 2022, vol. 12 (4), 1853, ISSN 2076-3417, DOI.org/10.3390/app12041853, 2022

Kuric, I., Klačková, I., Nikitin, Y.R., Zajačko, I., Císar, M., Tucki, K. (2021). Analysis of diagnostic methods and energy of production systems drives, Processes, Mdpi, 9, 843, DOI.org/10.3390/pr9050843, 2021

Kuric, I., Tlach, V., Císar, M., Ságová, Z., Zajačko, I. (2020). Examination of industrial robot performance parameters utilizing machine tool diagnostic methods. In International Journal of Advanced Robotic Systems, 17 (1), 2020, DOI 10.1177/1729881420905723, 2020

Landsat Levels of Processing | U.S. Geological Survey. Available at: https://www.usgs.gov/landsat-missions/landsat-levels-processing (Accessed June 14, 2022).

Laššák, M., Draganova, K., Blišťanová, M., Kalapoš, G. and Mikloš, J. (2020). "Small UAV Camera Gimbal Stabilization Using Digital Filters and Enhanced Control Algorithms for Aerial Survey and Monitoring." Acta Montanistica Slovaca 25, no. 1 (2020).

Khalilova, H. Kh. (2014) The Impact of Oil Contamination on Soil Ecosystem. Biological and Chemical Research, 2015, 133-139 (online). Available at http://www.ss-pub.org/wp-content/uploads/2015/03/4-BCR-E20141216-01.pdf (Accessed: 14 June 2022)

Muravev, V. V., Muraveva, O. V., Volkova, L. V., Sága, M., Ságová, Z. (2019). Measurement of Residual Stresses of Locomotive Wheel Treads During the Manufacturing Technological Cycle. Management systems in Production Engineering, 27 (4) 2019, DOI 10.1515/mspe-2019-0037, 2019

Pałaś, K.W. and Zawadzki, J., 2020. Sentinel-2 imagery processing for tree logging observations on the Białowieża Forest World Heritage Site. *Forests*, 11(8), p.857.

Pivin, M., Helsen, S., and Cuyvers, L. (2014). Feasibility study concerning remediation and rehabilitation of industrial polluted lands on the Absheron Peninsula, Republic of Azerbaijan. Geophysical Research Abstracts (16), EGU2014-10960 (online). Available at https://meetingorganizer.copernicus.org/EGU2014/EGU2014-10960.pdf

Saga M., Blatnicka M., Blatnicky M., Dizo J., Gerlici J. (2020). Research of the Fatigue Life of Welded Joints of High Strength Steel S960 QL Created Using Laser and Electron Beams, Materials, vol.13 (11), Article No. 2539, DOI 10.3390/ma13112539, 2020

Saga M., Blatnicky M., Vasko M., Dizo J., Kopas P., Gerlici J. (2020). Experimental Determination of the Manson-Coffin Curves for an Original Unconventional Vehicle Frame. Materials, vol.13 (20), Article No. 4675, DOI 10.3390/ma13204675, 2020

Saga M., Jakubovicova L. (2014). Simulation of vertical vehicle non-stationary random vibrations considering various speeds, Scientific Journal of Silesian University of Technology-Series Transport. Vol. 84, pp. 113-118, 2014

Saga, M., Vasko, M. (2009). Stress sensitivity analysis of the beam and shell finite elements. Komunikacie, vol. 11 (2), pp 5-12, ISSN 1335-4205, 2009

Saga M., Vasko, M., Pechac, P.(2014). Chosen numerical algorithms for interval finite element analysis. Modelling of Mechanical and Mechatronic Systems, MMaMS 2014, Vysoké Tatry, Slovakia, 25-27 nov. 2014, Procedia Engineering, vol. 96, pp. 400-409, DOI 10.1016/j.proeng.2014.12.109, 2014

Sapietova, A., Saga, M., Novak, P., Bednar, R., Dizo, J. (2011). Design and Application of Multi-software Platform for Solving of Mechanical Multi-body System Problems. Mechatronics: Recent Technological *a*nd Scientific Advances. 9th International Conference on Mechatronics, Warsaw, Poland, sep. 21-24, 2011, pp. 345-354, 2011

Segota, SB., Andelic, N., Lorencin, I., Saga M., Car, Z. (2020). Path planning optimization of six-degree-of-freedom robotic manipulators using evolutionary algorithms. International journal of advanc*ed robotic systems, vol.17 (2)*, DOI 10.1177/1729881420908076, 2020

Sentinel-2: Satellite imagery, Overview, and characteristics. Earth Observing System. Available at: https://eos.com/find-satellite/sentinel-2/ (Accessed June 14, 2022).

Sharov, P., Abbasov, R., and Temnikova, A. (2019). Remediation of soil contaminated with persistent organic pollutants in Sumgait, Azerbaijan. Environmental monitoring and assessment, 191(7), 464. https://doi.org/10.1007/s10661-019-7560-7

The Sentinel missions. ESA. Available at: https://www.esa.int/Our_Activities/Observing_the_Earth/Copernicus/Overview4 (Accessed June 14, 2022)

Saga M., Blatnicka M., Blatnicky M., Dizo J., Gerlici J. (2020). Research of the Fatigue Life of Welded Joints of High Strength Steel S960 QL Created Using Laser and Electron Beams, Materials, vol.13 (11), Article No. 2539, DOI 10.3390/ma13112539, 2020

Urban, R., Štroner, M., Blistan, P., Kovanič, Ľ., Patera, M., Jacko, S., Ďuriška, I., Kelemen, M. and Szabo, S. (2019) The Suitability of UAS for Mass Movement Monitoring Caused by Torrential Rainfall—A Study on the Talus Cones in the Alpine Terrain in High Tatras, Slovakia, ISPRS International Journal of Geo-Information, 8(8), p. 317. doi: 10.3390/ijgi8080317.